APPLICATIONS OF NASTRAN IN GUST RESPONSE ANALYSIS AT NORTHROP

Ashok K. Singh

SUMMARY

A comprehensive gust response analysis has been performed on a complete model of an airplane using the NASTRAN aeroelastic package by the Advanced Structural Computer Methods (ASCM) group at Northrop. Earlier the same model was used to perform subsonic flutter analysis of the airplane using the computer program. Both the random and discrete gust response analyses have been performed including the control system dynamics in the problem. On a large aircraft gust response analysis including the flexible modes of the vehicles is a major design task. On a light weight fighter aircraft the analysis is primarily performed in order to study the ride quality and to provide the frequency of exceedance curves for the control surface hinge moments and some selected dynamic loads for static and fatigue analysis.

INTRODUCTION

The NASTRAN finite element program has been used at Northrop since 1972. The ASCM group has been actively evaluating and exercising the various NASTRAN dynamics analysis features and the aeroelastic package for several months. Integrated NASTRAN structural analysis combining static and dynamic analysis, e.g., flutter and gust, is the planned goal at Northrop. In order to achieve this end, a common structural model throughout an engineering project must be used. This practice is also expected to minimize the use of inconsistent structural data and unnecessary data handling among the various engineering disciplines.

Symmetric response analysis is evaluated in two applications to the complete airplane aeroelastic model. The analyses are random response to atmospheric turbulence and transient response to a discrete gust. The structural and aerodynamic models are the same as that used in the flutter analysis as presented in Reference 1.

The gust response analysis by NASTRAN can only be performed with the aerodynamic forces computed by the Doublet-Lattice Method. Supersonic gust response capability has not been provided. Spacewise variation of the gust velocity is not allowed in the present NASTRAN formulation but should be considered for future development. The gust velocity normal to the free stream velocity is taken as an additional source of downwash in the computation of the aerodynamic forces. The standard forms of power spectrum of the atmospheric turbulence available in NASTRAN are Von Karman and Dryden. However, provision is made to use any other form of spectrum by the means of tabular input. In the case of the random gust analysis, the frequency response, power spectral density, root

mean square value and the frequency of zero crossing, N_o, of the response are output. A post processor can be easily written in order to compute the $\bar{A}$ and frequency of exceedance N(y) of the response. A procedure of weighting the aerodynamic forces to match measured data on each panel must be developed.

The discrete gust analysis is performed by the Fourier method. First, the time varying loads are transformed into the frequency domain by Fourier series or Fourier integrals. Second, the responses computed in the frequency domain are converted into the time domain by inverse Fourier transform methods. Three approximate methods are available in order to evaluate the inverse.

A flight control system is incorporated in the NASTRAN model that utilizes a Ride Improvement Mode System (RIMS) and pitch Control Augmentation System (CAS). A dedicated accelerometer and pitch rate gyro near the pilot station are chosen to measure acceleration and pitch rate which are fedback as the control signal in order to actuate the flaperon and stabilator (Figure 1).

To obtain satisfactory ride qualities during low altitude high speed flight, extensive effort has been expended in the development of a ride improvement system. The system tries to maintain a constant value of lift for changes in angle-of-attack due to turbulence. This is performed by sensing the load factor at the pilot station and using that as a control signal to command the high rate flaperons, so that the flaperons can minimize the turbulence-induced incremental load factor at the pilot station.

Operating in parallel with the ride mode is the CAS which uses a blend of load factor and pitch rate to maintain aircraft stability while trying to minimize uncommanded pitch rate and load factor.

With the advent of the control configured vehicle, today's control system engineer must have a thorough knowledge of aeroservoelastic behavior of the flying machine. The design of the filters in the feedback loop cannot be completed without the knowledge of elastic and aeroelastic characteristics of the modern aircaraft. A new engineering discipline of aeroservoelasticity is emerging which will play a prominent role in the early design phases of an integrated control system.

SYMBOLS

$\bar{A}$ Ratio of root-mean-square value of load to root-mean-square value of gust velocity

b_1 b_2 Intensity parameters in the expression for probability of σ_a

$H_{ja}(\omega)$ Frequency response due to the gust excitation

N_o Average number of zero crossings with positive slope, per unit time

$N(y)$ Number of exceedances of the indicated value of y per unit time

P_1, P_2 Fractions of total flight time in non-storm and storm turbulence respectively

$S_a(\omega)$ Power spectral density of gust velocity

$S_j(\omega)$ Power spectral density of response

σ_r Root-mean-square value of response quantity

σ_a Root-mean-square value of gust velocity

ω Circular frequency

ω_c Cutoff frequency beyond which aeroelastic responses are no longer significant in turbulence

NASTRAN GUST RESPONSE ANALYSIS

The gust response analysis is performed on a complete aircraft in the following steps:

- Random response to Von Karman gust spectrum without control system interaction
- Random response to Von Karman gust spectrum with control system interaction
- Transient response to a discrete gust with control system interaction

RANDOM RESPONSE ANALYSIS

A NASTRAN beam element model of a complete airplane was used to perform the gust response analysis. The airplane with a tip store, launcher rail, wing, flaperon, fuselage, fin with rudder and horizontal stabilizer was modeled as finite beam elements as shown in Figure 2. The store and launcher rail assembly was tied to the wing tip by rigid elements which may be modified to possess elastic properties. The wing root and fin root flexibilities were modeled by lumped springs, which may be made more complex as the finite element model of the airplane is developed. The horizontal stabilizer root stiffness is a general element accounting for the spindle and the actuator assembly flexibilities. Mass properties were input on lumped mass element cards.

A doublet-lattice finite element program was used to represent the aerodynamics of the vehicle as shown in Figure 3. The wing with the launcher rail, fin with the rudder and horizontal stabilizer are represented as lifting surface elements. The fuselage is represented as slender body and interference elements. In the present analysis, the aerodynamic induction effect among all the elements is considered. The wing, horizontal stabilizer and fin are

divided into 145, 20 and 20 micro lifting surface elements, respectively. The fuselage is divided into 14 slender body elements. There are 11 interference elements on the fuselage.

A complicated network of linear spline functions is used to relate the modal deflections to each of the aerodynamic element deflections. Five distinct splines were used for the wing, rail and flaperon panels, two for the horizontal stabilizer, three for the fin with rudder, two for the fuselage and one for the store.

The flight control system is represented in the model as 9 extra points and 2 scalar points with their coefficients in the mass, damping and stiffness matrices in order to represent the filters in the feedback loop. The two scalar points are the relative rotations of the flaperon and the stabilator. Constraint forces in the equations of motion due to the control laws are introduced by the Lagrange multiplier technique. An accelerometer and a pitch rate gyro are located near the pilot station in order to measure the airplane responses. The measured data are fedback in order to activate RIMS and CAS laws, which control the aircraft response.

The unsteady aerodynamics for Mach 0.8 and sea level is generated for eight reduced frequencies using the Doublet-Lattice Method available in NASTRAN. Symmetric flight condition is considered in the analysis. Three symmetric rigid body modes and twenty-two elastic modes are selected to generalize the aerodynamic forces. Only the modal method of aeroelastic response computation is available in the program. Generalized aerodynamic forces at other intermediate reduced frequencies are computed by means of a linear spline interpolation routine.

The gust response analysis of a light weight fighter considered in this problem is primarily performed in order to study the ride quality of the vehicle. In order to increase the survivability of modern fighter aircraft, new emphasis is being given to the capability of low-altitude high-speed penetration. For such an aircraft, the low-wing loading/high-lift curve slope which maximizes turn rate capability and maneuverability essential for survival in air combat also tends to deteriorate the ride quality during high-speed penetration. This can lead to reduced mission success in attacking heavily defended ground targets, or in the worst case even mission failure.

For the evaluation of ride quality through turbulence, $\bar{A}$ is used. $\bar{A}$ is the root-mean-square (rms) of the response divided by the rms gust level in feet per second (fps) as defined in Equation 1.

$$\bar{A} = \left[\frac{\int_0^{\omega_c} \left| H_{ja}(\omega) \right|^2 S_a(\omega) d\omega}{\int_0^{\infty} S_a(\omega) d\omega} \right]^{\frac{1}{2}} = \frac{\sigma_r}{\sigma_a} \qquad (1)$$

To simulate turbulence the Gaussian Von Karman model was used with an rms gust intensity level of one fps (References 2 & 3). The scale of turbulence used in the analysis is 500 feet. In order to compute the $\bar{A}$ of the pilot acceleration response a cutoff frequency of 30 Hz was used.

The characteristic frequency, N_o, is the radius of gyration of the response power-spectral density curve with respect to zero frequency (Equation 2).

$$N_o^2 = \frac{\left(\int_o^\infty (\omega/2\pi)^2 S_j(\omega)\, d\omega\right)}{\left(\int_o^\infty S_j(\omega)\, d\omega\right)} \qquad (2)$$

NASTRAN computes σ_r and N_o by the solution of the airplane equations of motion. A post processor may be written in order to compute $\bar{A}$ and load exceedances N(y). Frequency of exceedance, N(y), is the number of exceedances of y per unit time or distance flown, where y is any response quantity (Equation 3).

$$N(y) = N_o \left[P_1 \exp\left(-\frac{y}{\bar{A}b_1}\right) + P_2 \exp\left(-\frac{y}{\bar{A}b_2}\right)\right] \qquad (3)$$

The first fuselage bending mode, whose frequency is 9.5 Hz, is shown in Figure 4. Note that the pilot station coincides with the forward node point. Transfer functions and power spectral densities of the aircraft with and without the active controls are given in Figures 5 thru 12. Most of the response at the pilot station without the active controls is due to the short period and the first wing bending modes. When the RIMS and CAS are incorporated in the equations of motion, the response due to the short period mode is markedly lowered but some of the high frequency responses are amplified. The net result in the $\bar{A}$ of the pilot station acceleration is a 37% reduction due to the control system dynamics, while the N_o values are higher. If the visceral response of the pilot is only frequency dependent, the ride quality is significantly improved by the RIMS and CAS system used in the analysis. Most of the improvement in the ride quality is due to the RIMS interaction alone.

The restart capability of NASTRAN has been used to study the ride quality by varying the gains in the feedback loops. Similar restarts may be made to vary the scale of turbulence or the gust spectrum at a fraction of the cost of the parent analysis.

TRANSIENT RESPONSE ANALYSIS

Due to the poor ride quality of the modern fighter aircraft a great interest has been generated in time domain analysis in parallel with the

frequency domain analysis in order to evaluate the handling quality. Transient analysis by a Fourier method is available in NASTRAN. The loads defined as a function of time are transformed into the frequency domain by Fourier transform methods.

In the present analysis a (1-Cosine) gust profile with a critical gradient of 12.5 chord is used. The maximum gust velocity in the profile is 50 ft/sec. The NASTRAN restart capability was used to tune the gust response by varying the critical gradient.

Using the Fourier method, the single gust profile is replaced by a series of pulses with a period of 20 seconds. The forcing function is zero for some time interval to allow for the decay of the responses. In order to evaluate the inverse transform equal frequency intervals, method 0, is used.

The time histories of the relative rotations of the flaperon and the stabilator are presented in Figures 13 and 14, respectively. The time history of the pilot station displacement is shown in Figure 15. Most of the pilot station response is due to the short period mode with a first wing bending mode contribution superimposed upon it, as shown by the magnified view in Figure 16. The responses are well decayed before the next gust pulse hits the aircraft.

CONCLUSIONS

This paper shows that NASTRAN is an extremely effective tool for aeroelastic analysis.

A subsonic gust response analysis has been performed in order to evaluate its usefulness in the flight vehicle system design. In an earlier evaluation, NASTRAN flutter analysis capability has been found to be very satisfactory as it provides several state-of-the-art methods and also saves considerable amount of man-hours by avoiding duplication of the structural model by the static and dynamics group (Reference 1). In the pre-NASTRAN era it has been a normal practice in many aircraft companies to model the vehicle structure separately in the stress, flutter and gust response groups. The aerodynamic model is also duplicated within the groups. A consistent and systematic method of incorporating control system dynamics in the various engineering disciplines is also lacking. With the advent of the control configured vehicle, a new engineering discipline of aeroservoelasticity is emerging in a dominant engineering role in the early design phases of the aircraft structure and integrated control system. NASTRAN aeroelastic package with its integrated stress, flutter, gust response, and control systems interaction is a very powerful structural analysis tool. It is well tailored for interactive graphics environments with data base management systems. With the emphasis on aeroelastic tailoring and structural optimization in the aircraft design, NASTRAN is amply ready to play a central role.

The gust response analysis performed in this paper on a light weight fighter has given a great insight in the active control system design. The use of RIMS and CAS systems reduce the $\bar{R}$ of the pilot station acceleration responses by 37%. The random gust response due to the short period mode is

significantly lowered. However, the response due to the structural modes either remains unchanged or some of the higher frequency modes are attenuated. This means that the present RIMS and CAS feedback loop gains and filters have to be modified to suppress the high frequency structural responses. This is an important revelation, which would have gone unnoticed in a customary rigid airplane control system analysis. Use of the active control system aggravates the dynamic loads on the flaperon, stabilator, etc., structures.

The transient response analysis of a fighter aircraft is also performed by NASTRAN to satisfy a point of view, which wants to look at the time history of the pilot response in addition to the frequency related behavior studied by the random gust analysis. It is quite possible that the pilot's discomforts are related to the jerks he feels while flying over the discrete impulses of the gust rather than a visceral response based on the frequency contents of the gust induced excitation. More work has to be done in this area in which NASTRAN can be used as a major design tool.

In all aeroelastic analyses, the checkpoint and restart capability should be used in order to study the influence of changing the scale of turbulence, gust spectrum, structural damping, feedback loop gains and filters, etc., on the responses. Restart procedure is very cost effective and should be further improved.

Generation of aerodynamic influence coefficients and a procedure to weight the aerodynamic forces and moments on each of the panels should be provided in order to match the test data. Additional plot capability should be provided to plot all the aerodynamic elements, spline fitted modes and aerodynamic pressure distributions. For the design of large aircraft, spacewise variation of the gust spectrum should be incorporated and coherency, cross-correlation and cross-spectral density should be calculated as gust response analysis. Mode acceleration method of response computation should be provided in the rigid format. A method of computing shear, bending moment and torque at wing stations or fuselage stations, etc., and plotting them as response quantities is also needed.

REFERENCES

1. Singh, A. K., "Applications of NASTRAN in Aeroelastic Analyses at Northrop," Proceedings of the MSC/NASTRAN User's Conference, March 15-16, 1979; and Finite Element News, July 1979.

2. Rodden, W. P., Harder, R. L., and Bellinger, E. D., "Aeroelastic Addition to NASTRAN," NASA Contractor Report 3094, March 1979.

3. Anon., "MSC/NASTRAN Aeroelastic Supplement," 1979.

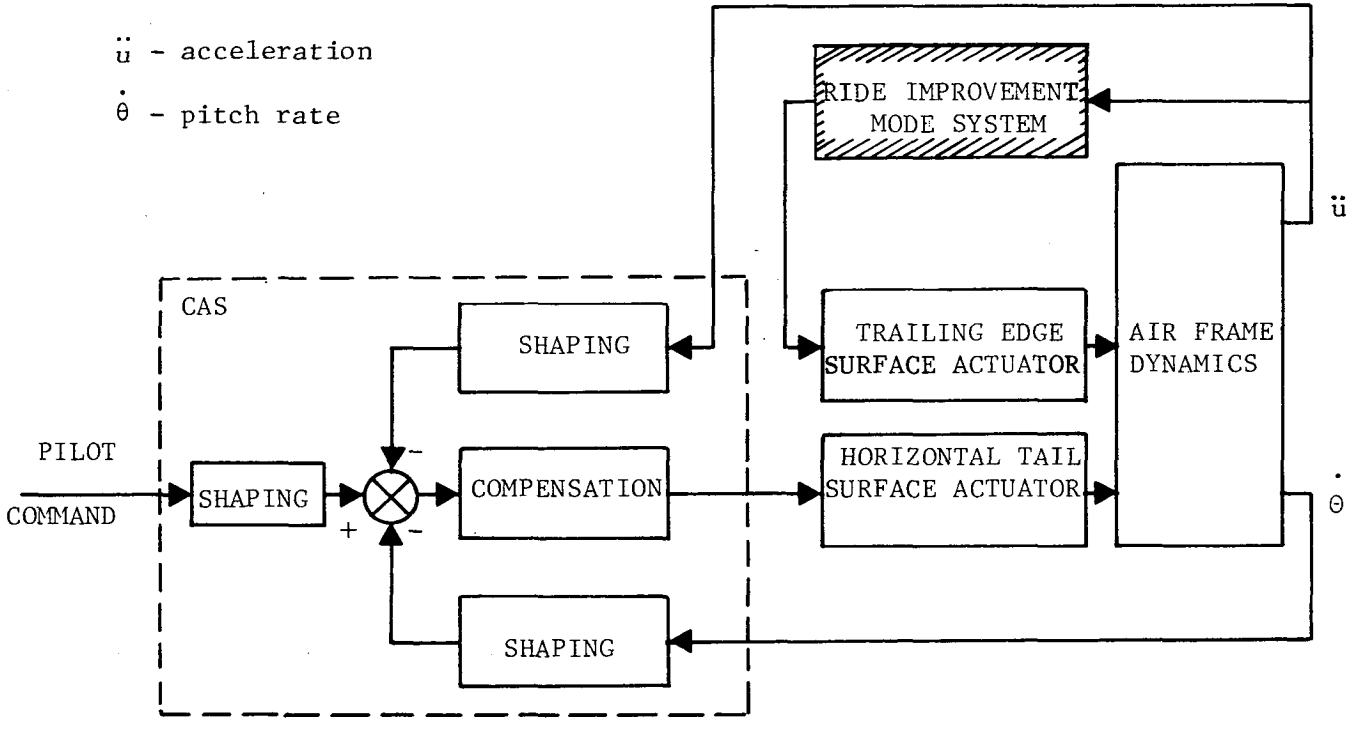

Figure 1. Longitudinal Control System Concept

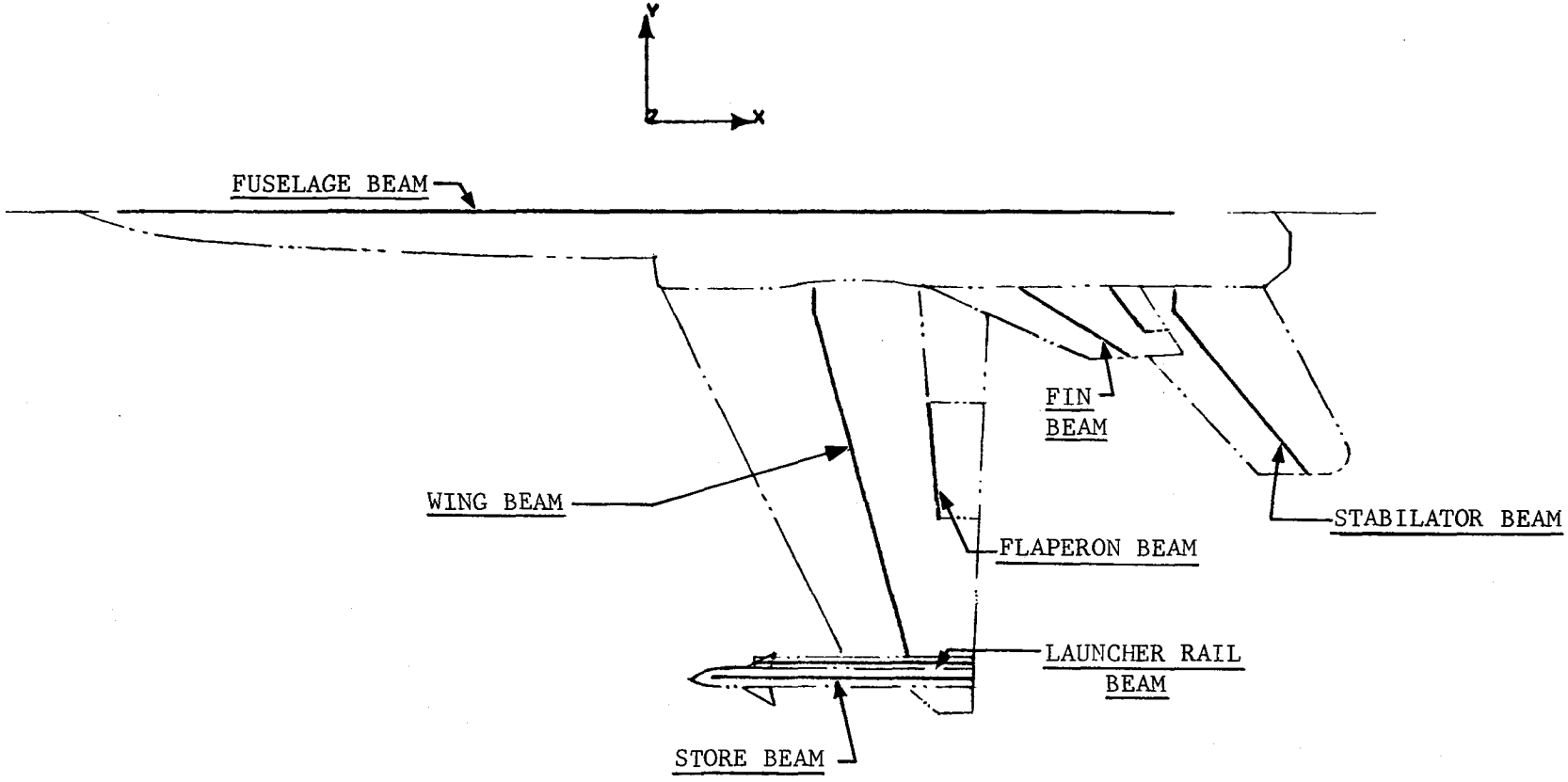

Figure 2. Complete Airplane Structural Model - NASTRAN

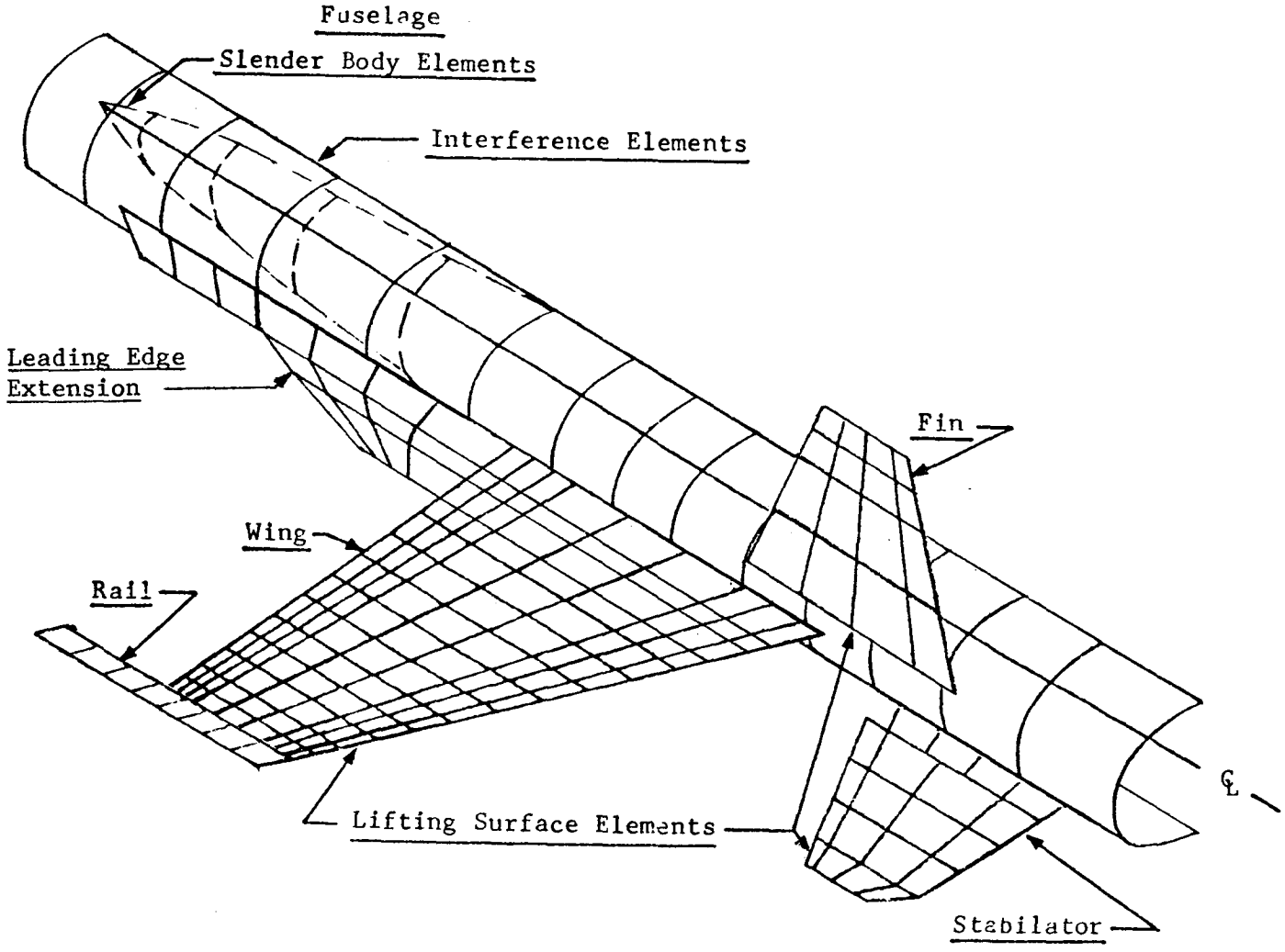

Figure 3. Complete Airplane Aerodynamic Model - NASTRAN

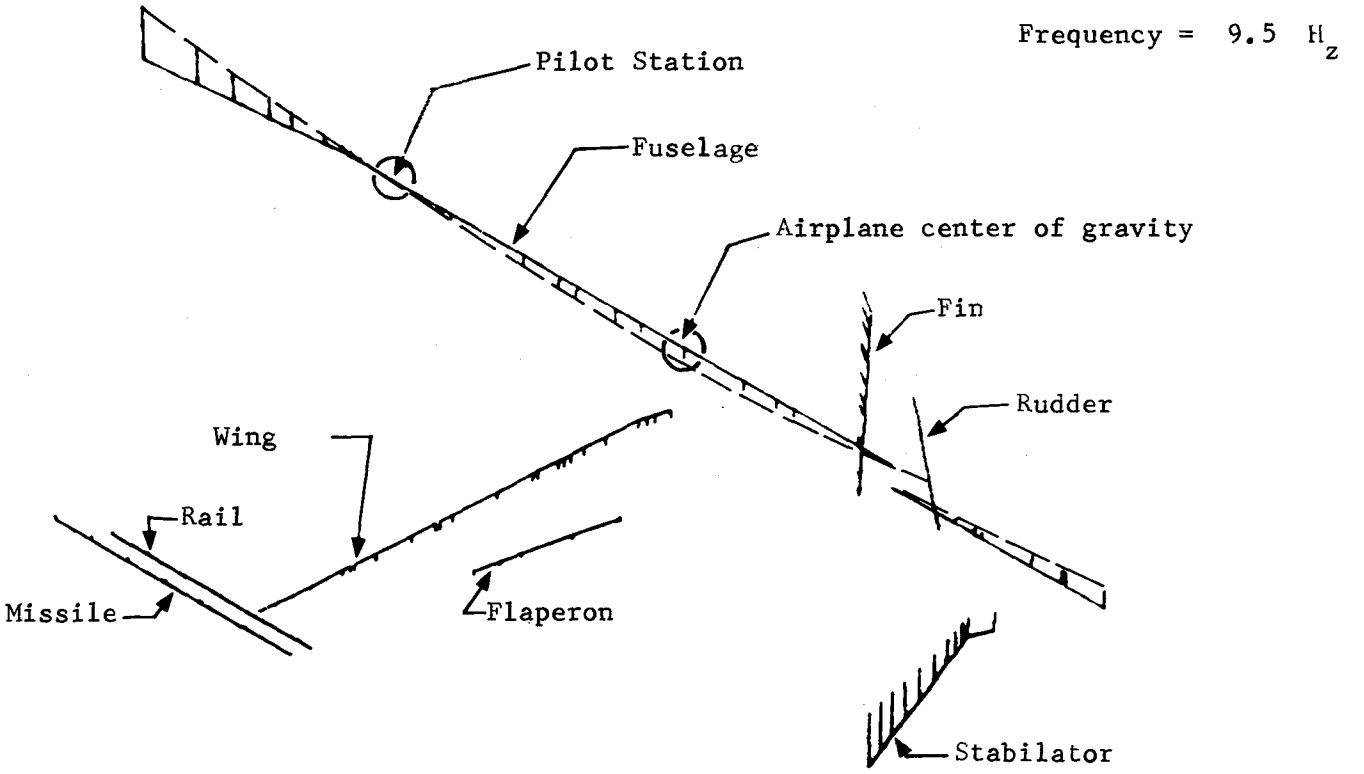

Figure 4. Fuselage Vibration Mode

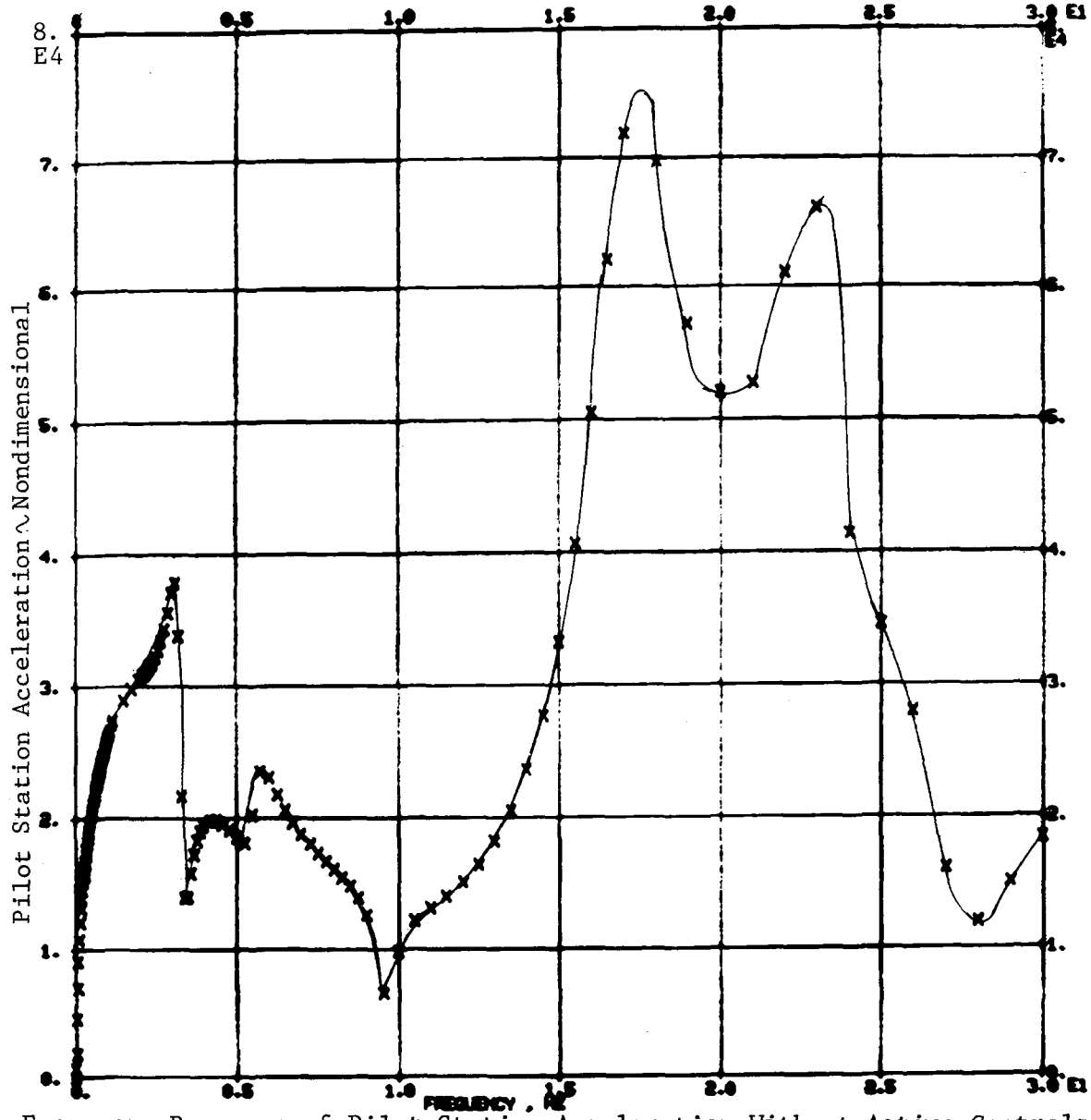

Figure 5. Frequency Response of Pilot Station Acceleration Without Active Controls

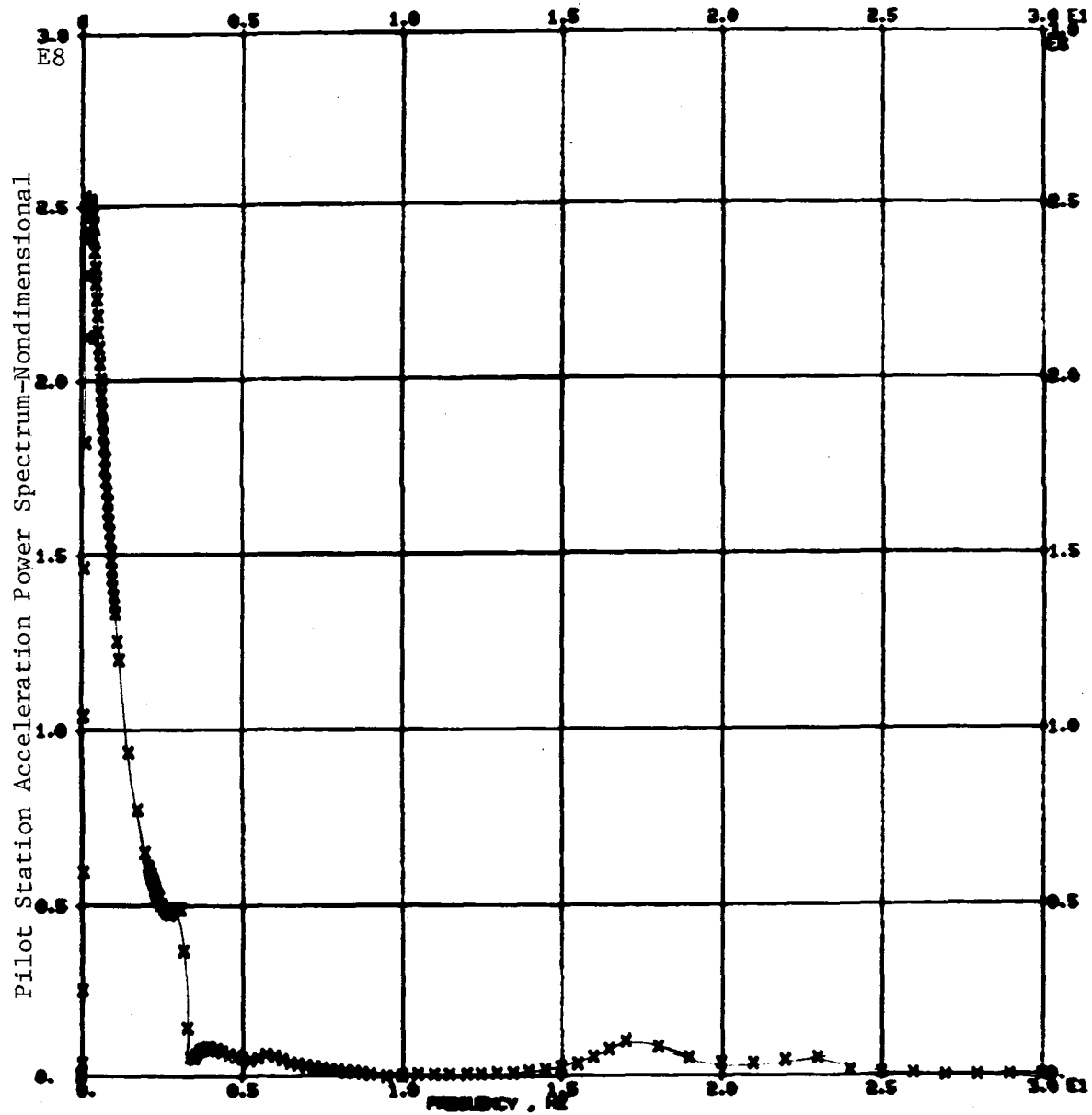

Figure 6. Power Spectral Density of Pilot Station Acceleration Without Active Controls

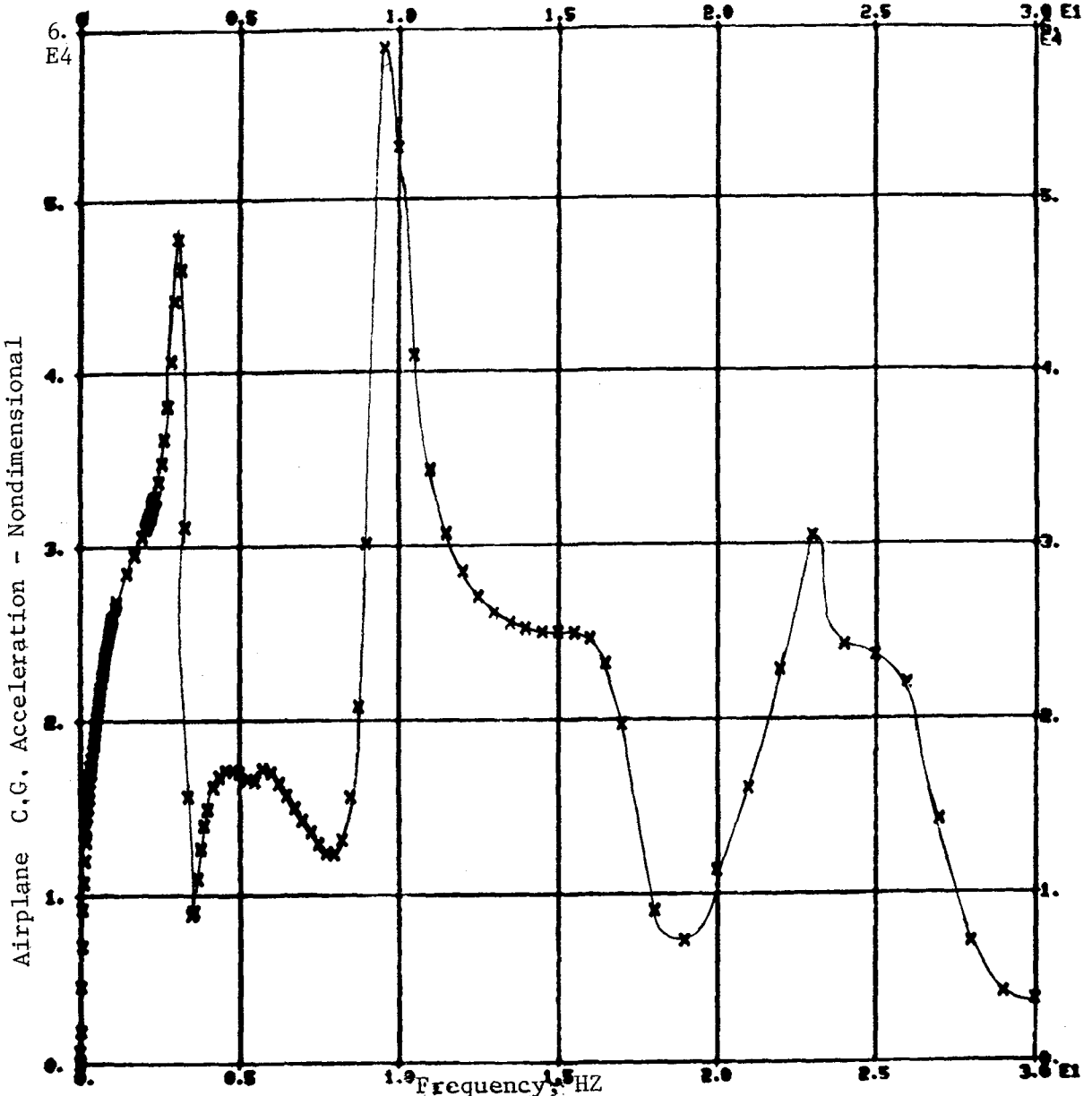

Figure 7. Frequency Response of Airplane C.G. Acceleration Without Active Controls

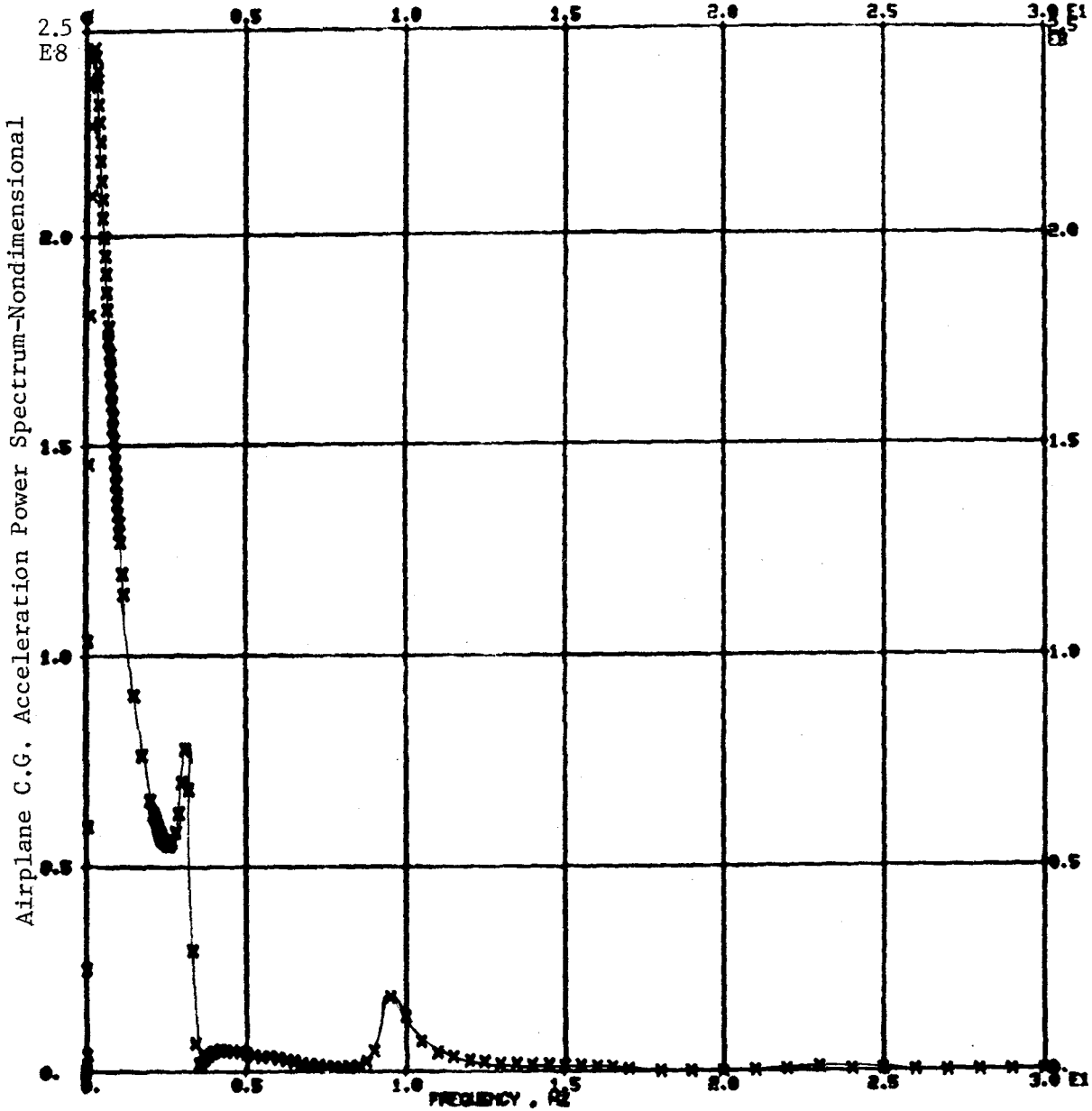

Figure 8. Power Spectral Density of Airplane C.G. Acceleration Without Active Control

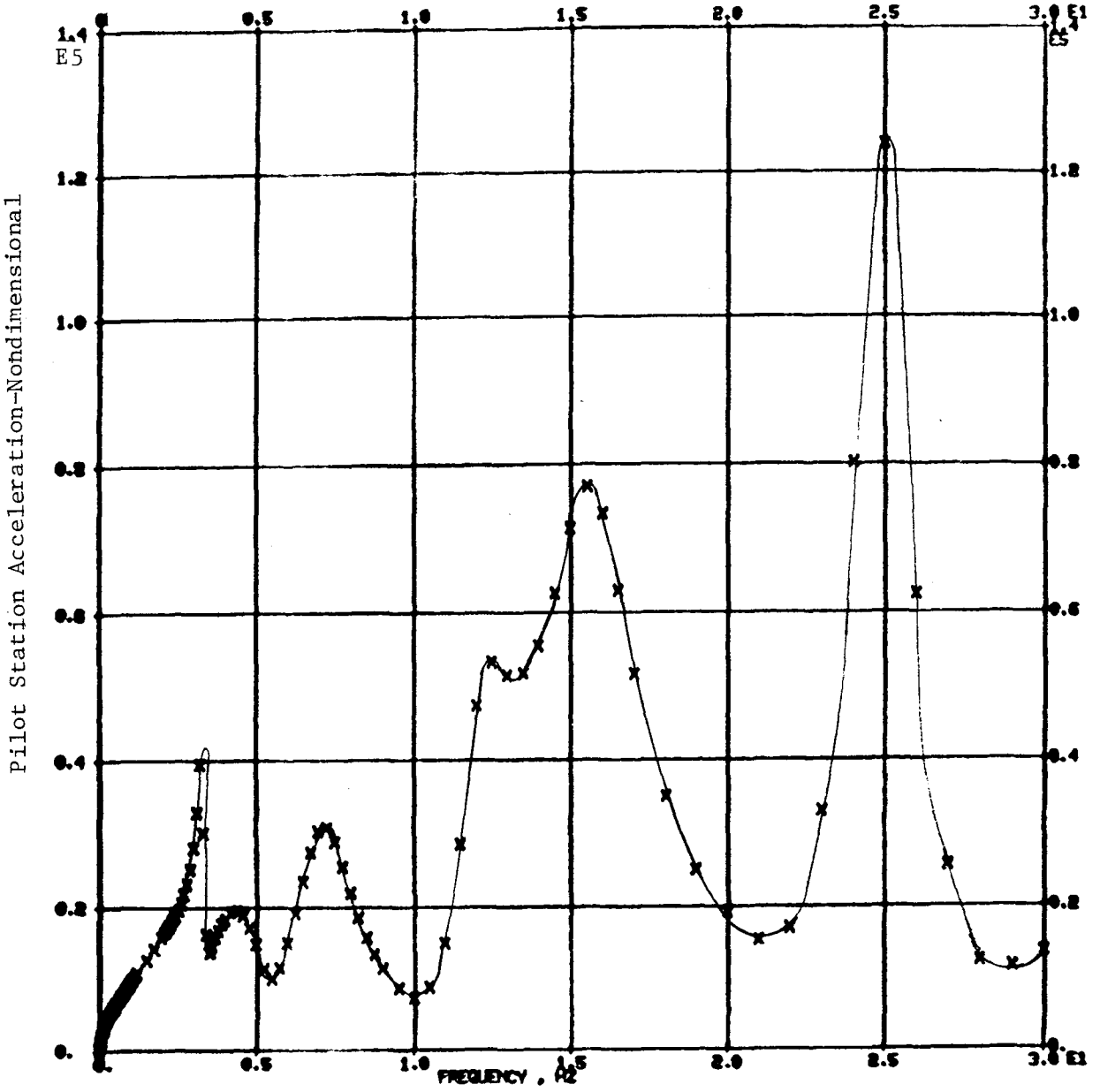

Figure 9. Frequency Response of Pilot Station Acceleration With Active Controls

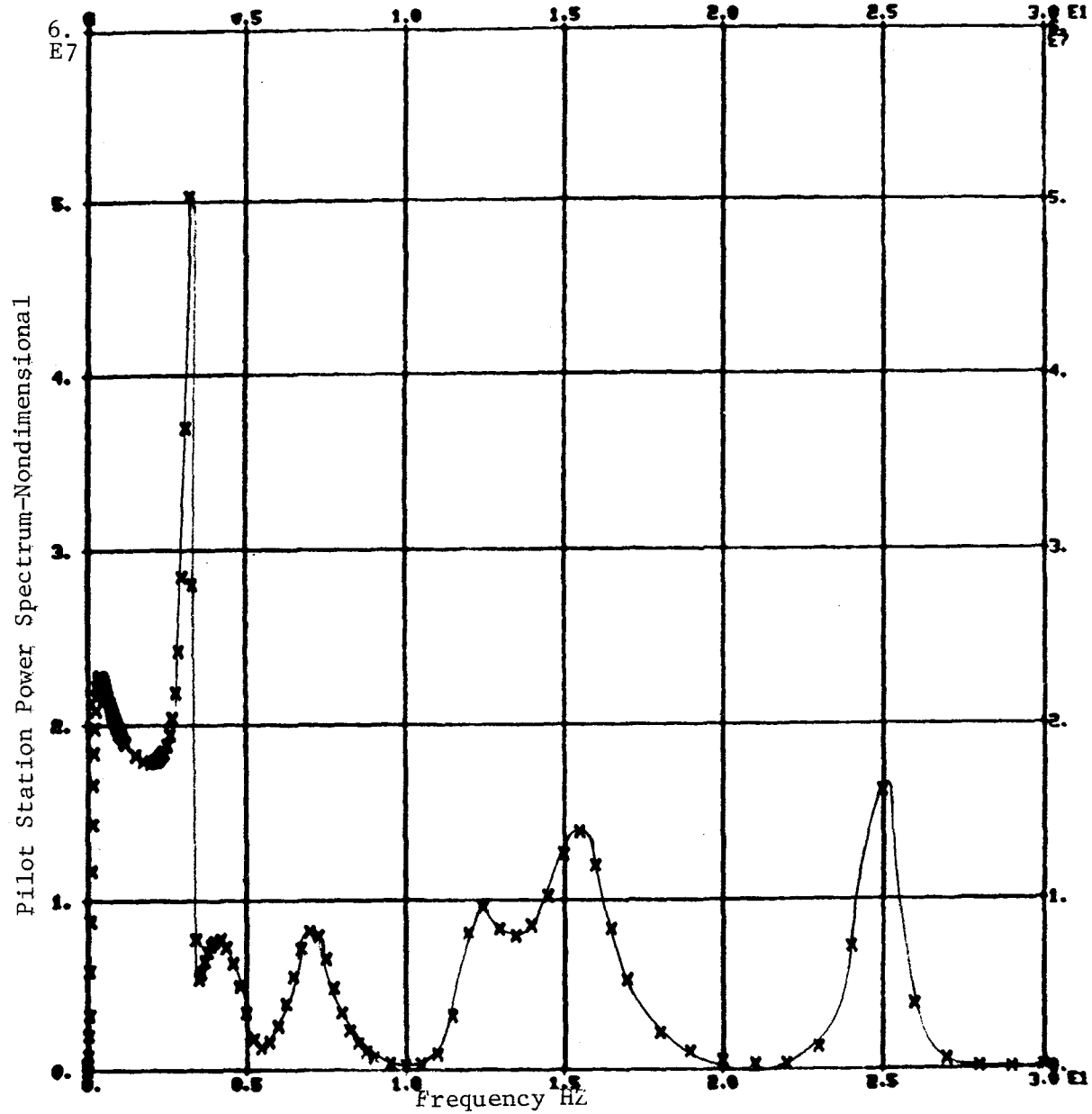

Figure 10. Power Spectral Density of Pilot Station Acceleration With Active Controls

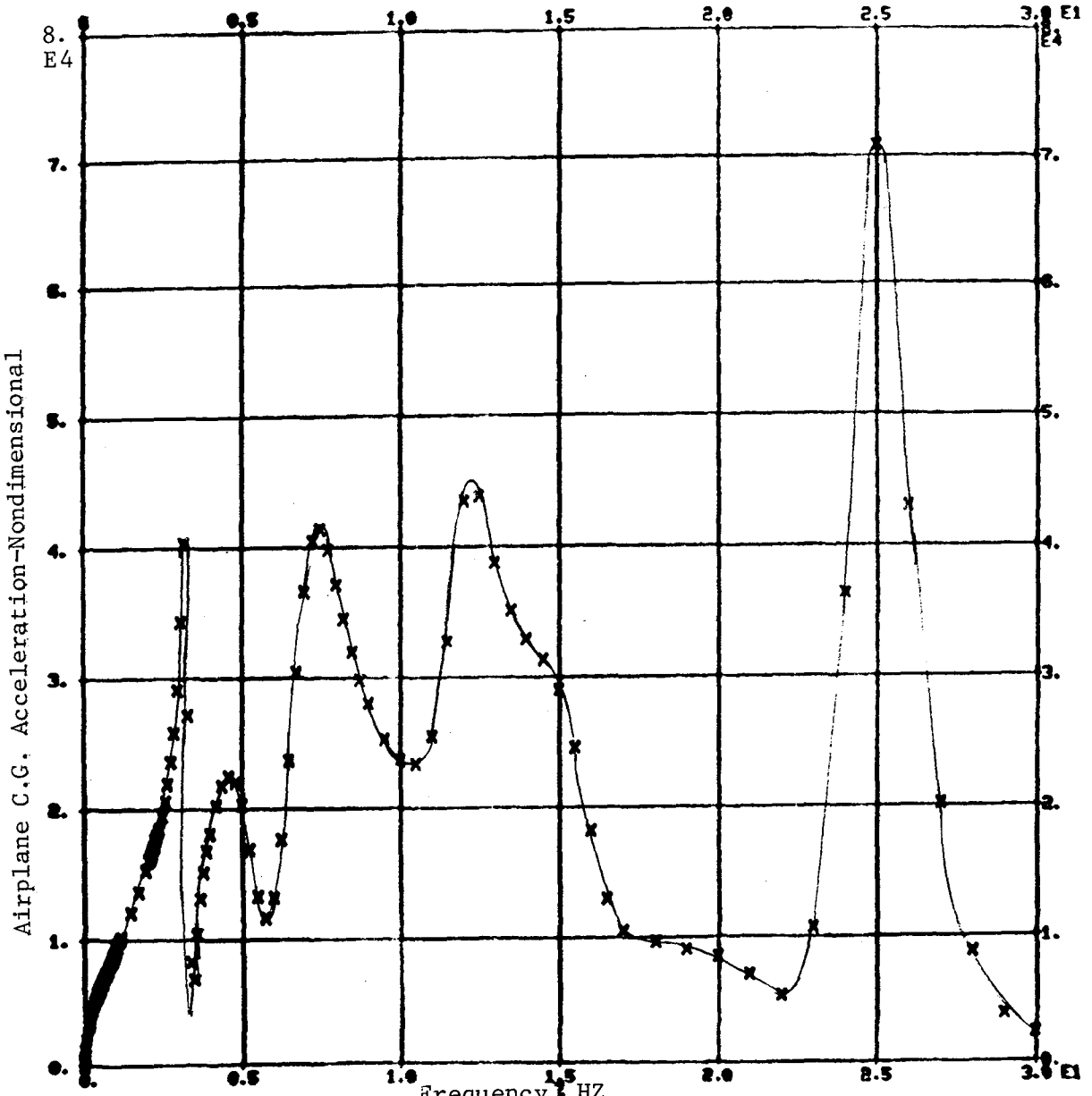

Figure 11. Frequency Response of Airplane C.G. Acceleration With Active Controls

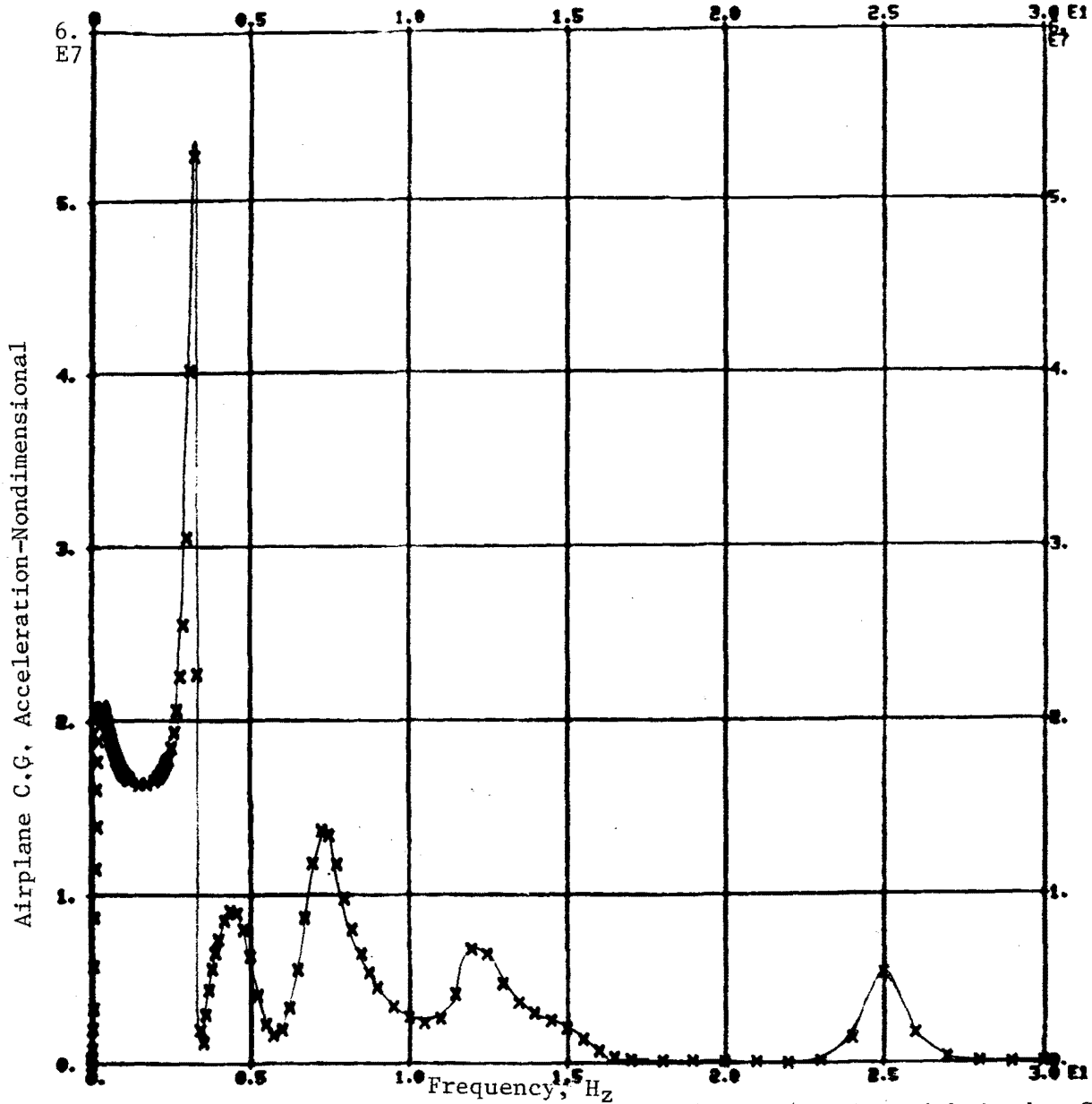

Figure 12. Power Spectral Density of Airplane C.G. Acceleration With Active Controls

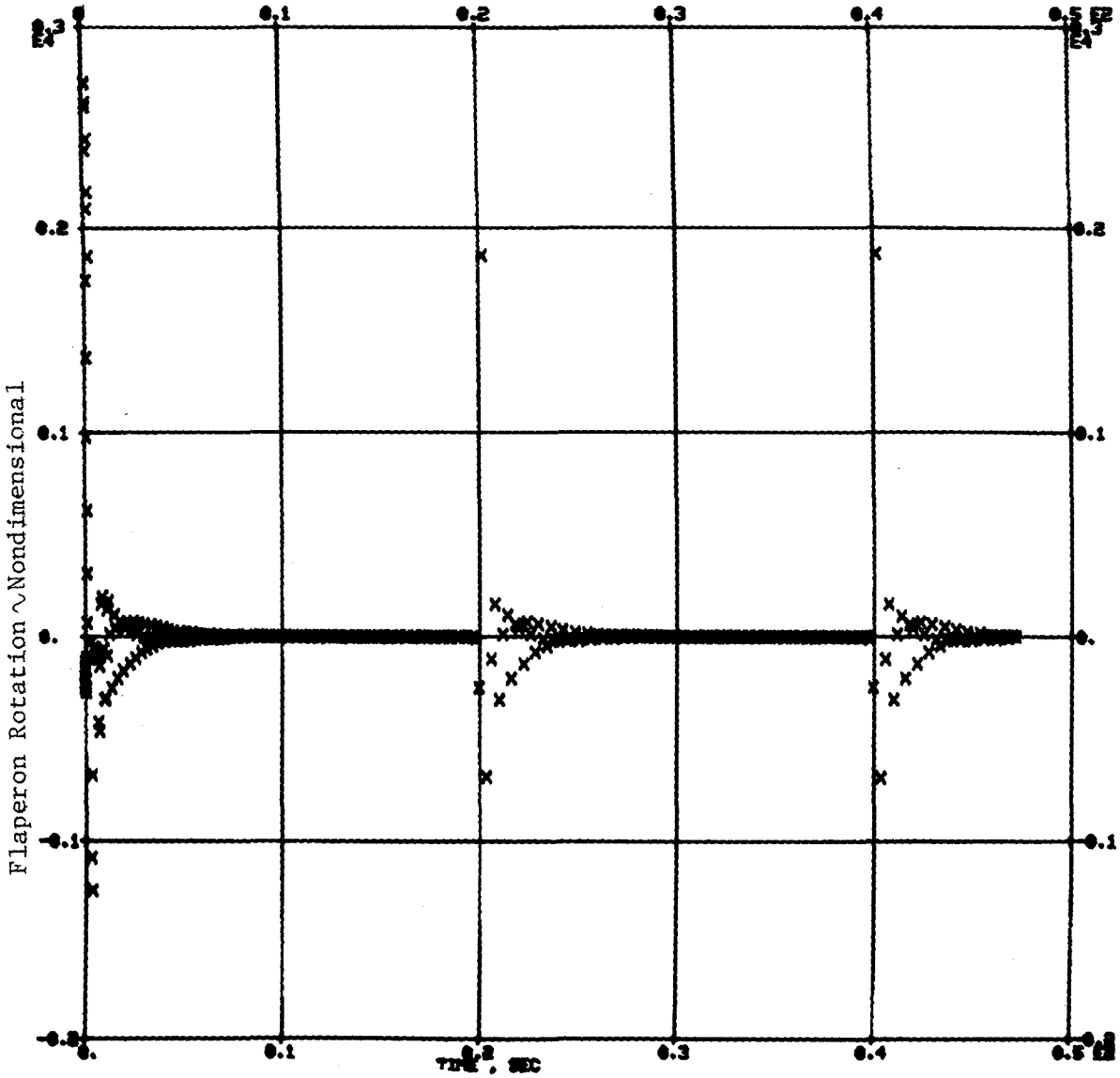

Figure 13. Time History of Flaperon Rotation With Active Controls

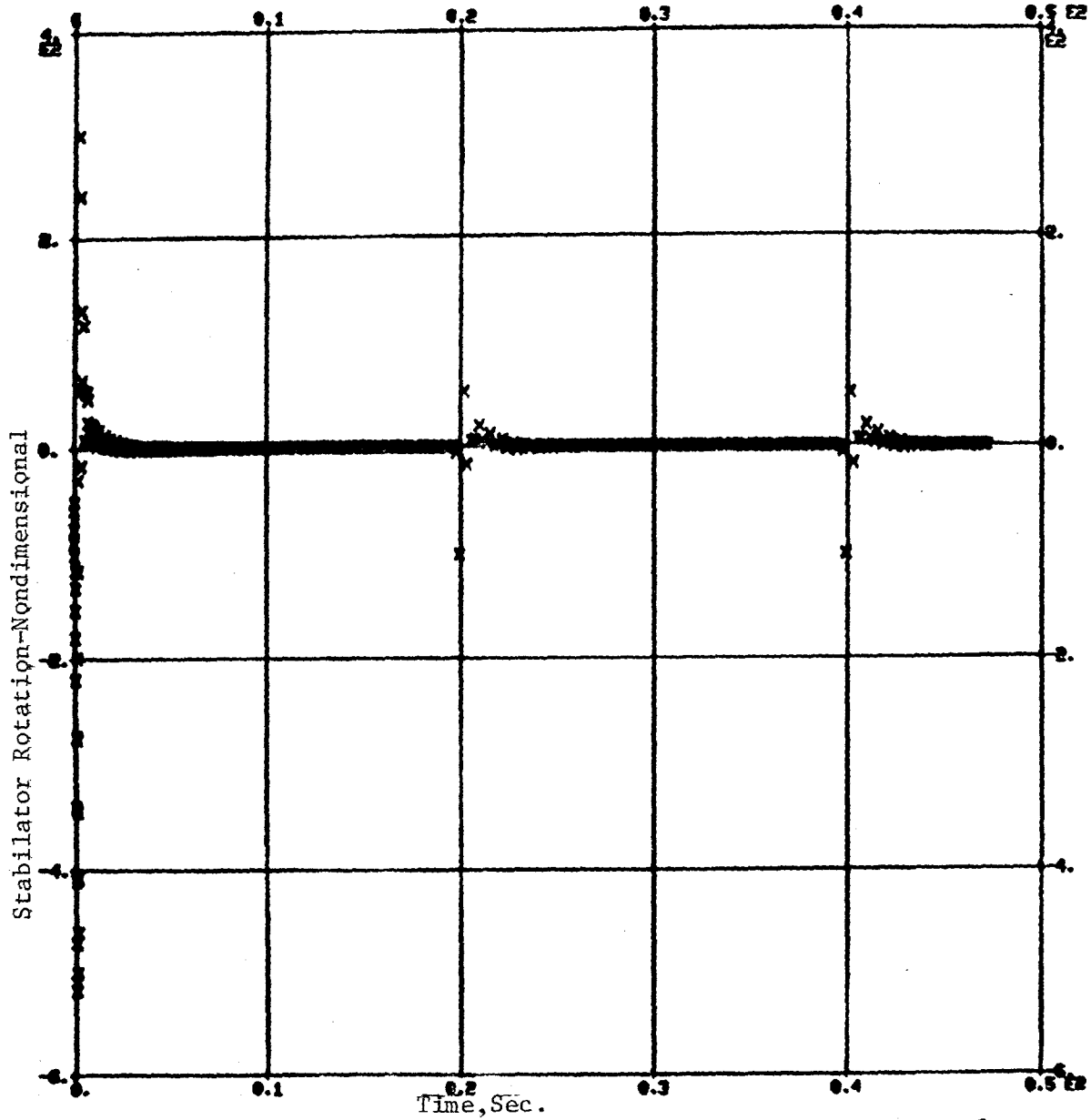

Figure 14. Time History of Stabilator With Active Controls

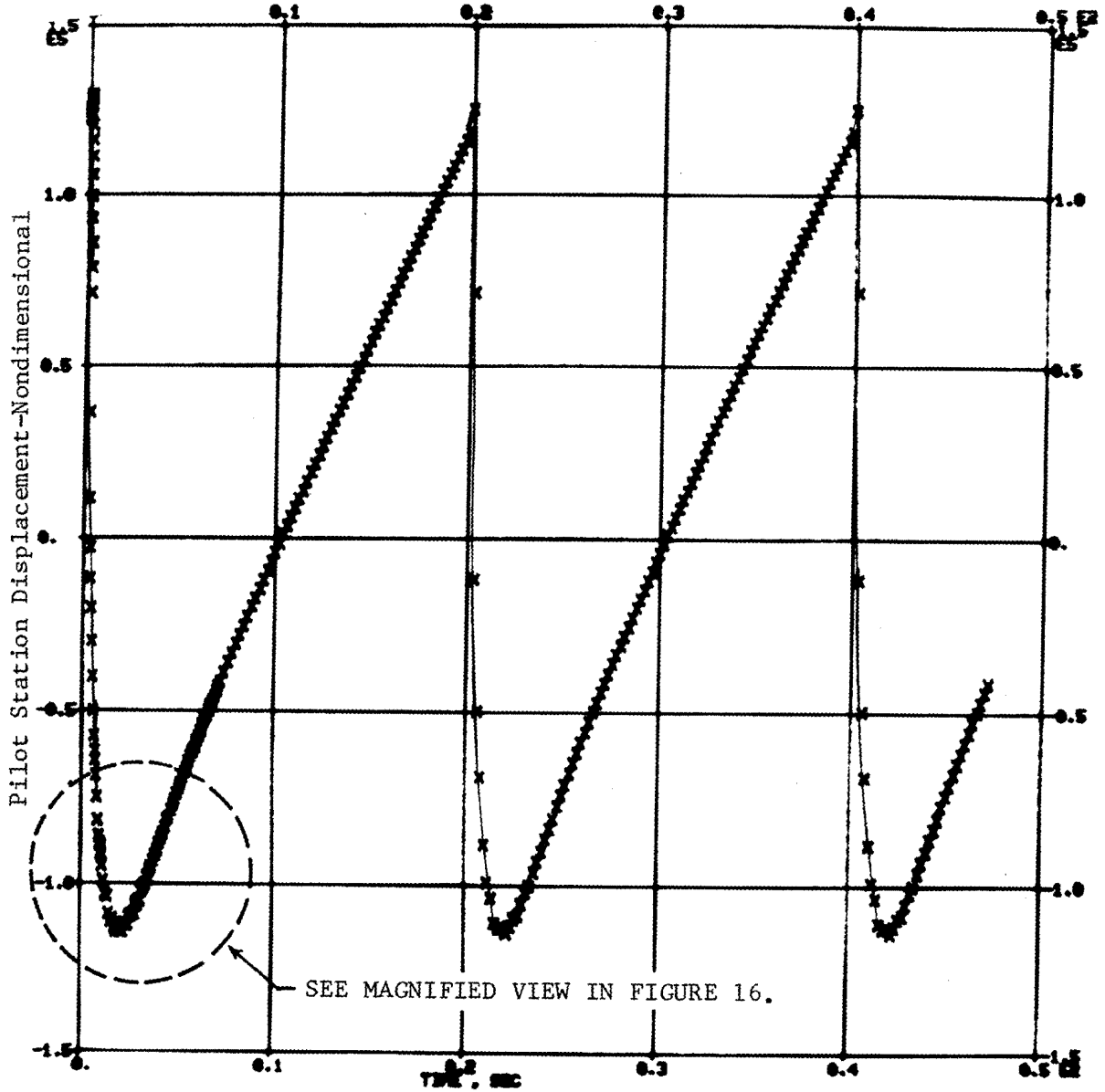

Figure 15. Time History of Pilot Station Displacement With Active Controls

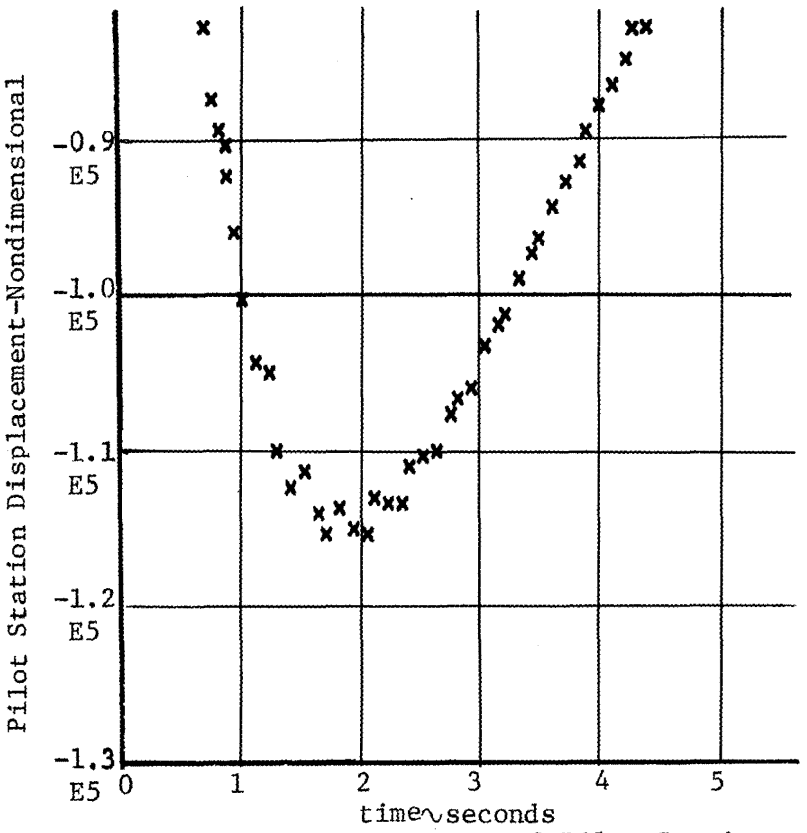

Figure 16. Time History of Pilot Station Displacement With Active Controls